Limnol. Oceanogr., 52(4), 2007, 1523–1532

Convergences and divergences and thin layer formation and maintenance

Mark T. Stacey[1]
Department of Civil and Environmental Engineering, University of California, Berkeley, California

Margaret A. McManus
Department of Oceanography, University of Hawaii, Manoa, Hawaii

Jonah V. Steinbuck
Environmental Fluid Mechanics Laboratory, Stanford University, Stanford, California

Abstract

The formation and maintenance of thin layers in the presence of turbulent diffusion is considered through the development of a formal framework that evaluates the balance between convergence mechanisms and the diffusive effects of turbulence. Turbulent diffusion acts to broaden layers, thus a convergence is required to produce a persistent and stable layer structure. Convergence mechanisms considered here include straining by a sheared velocity profile, organism motility, and particle buoyancy. The balance between each of these convergences and turbulent diffusion results in a scale estimate for the layer thickness that depends on local conditions. Comparison of these layer thickness scales for each of the three mechanisms enables us to evaluate which mechanism is likely to be dominant in particular situations. An example application of the framework is based on observations of thin layers in East Sound, Washington, for which we conclude that either the buoyancy or straining mechanism could contribute to the maintenance of the layer. Finally, the analytic framework itself provides insights into thin layer dynamics, including the prediction of a finite layer lifetime for shear-driven layers and the effects of mixing events on the convergence mechanisms acting to maintain the layers.

During the last two decades, technology has led to the discovery of previously undetected thin layers of biological organisms in the coastal ocean (Cowles et al. 1990; Cowles et al. 1993; Holliday et al. 1998). These layers are characterized by vertical thicknesses of the order of decimeters to meters, but have broad horizontal extent and are persistent in time (Rines et al. 2002; McManus et al. 2003). In recent work, Dekshenieks et al. (2001) have defined a criteria for a feature to be considered a thin layer that is based on the relative concentration of organisms in the layer and the thickness of the layer. Specifically, they argue that a thin layer must be $<$5-m thick, must be observable in multiple profiles, and must have an optical signal more than three times greater than the background signal.

In general, the observations of thin phytoplankton layers indicate that these layers are associated with physically stratified layers, which are generally stable to shear instabilities (McManus et al. 2003). Whereas low mixing levels could explain the persistence of layers, observations have indicated moderate turbulent levels associated with many layers (McManus et al. 2003). Further, the absence of mixing does not, by itself, explain the initial formation of the layer. Several mechanisms have been explored to explain the onset and maintenance of these layers. Recent work by Genin et al. (2005) established the ability of zooplankton to effectively maintain their position in the water column through directed swimming. Although it was unclear what the zooplankters were responding to in adjusting their swimming, the authors were able to establish the fact that these copepods could effectively counter vertical currents as large as 1 cm s^{-1}. Earlier work by Franks (1992) examined the potential for buoyancy to maintain the position of a phytoplankter along an isopycnal. In this case, individual phytoplankters are retained at an equilibrium density; displacements from this position are opposed by the buoyancy force acting on the phytoplankter. Finally, Franks (1995) proposed a shear-driven mechanism for layer formation that was based on pure straining of a patch of passive phytoplankton by the horizontal velocities induced by near-inertial internal waves. In each of these cases, the formation mechanism provides a convergence into a thin layer, which will act in opposition to diffusion by turbulent (or molecular) mixing.

In this article, we develop a framework that explicitly considers the competition between convergence and diffusion. Specifically, we present a scaling approach to examining the balance between various convergence mechanisms and diffusion of the layers. The resulting framework enables us to compare the relative importance of straining, motility, and buoyancy, including an evaluation of which mechanism is likely to dominate under given conditions.

[1] Corresponding author (mstacey@berkeley.edu)

Acknowledgments

The Office of Naval Research (N00014-04-1-0311) supported data analysis and manuscript preparation. Percy Donaghay, James Sullivan, and Tom Osborn helped with the East Sound data collection and analysis, and the insightful comments and suggestions of two anonymous reviewers significantly improved the manuscript.

Defining the convergence–diffusion balance

In order for a persistent and relatively coherent thin biological layer structure to be maintained, processes acting to expand and collapse the layer must be in balance. Here we will consider three candidate convergence mechanisms that would act to thin the layer: straining, motility, and buoyancy. In each case, as the layer is thinned by the convergence mechanism, turbulent diffusion becomes increasingly effective at broadening the layer (relative to the layer thickness), or at least maintaining the layer thickness and counteracting the effects of the convergence mechanism.

Defining the layer thickness as l, we define the net rate of change of the layer thickness as

$$\left(\frac{\partial l}{\partial t}\right)_{net} = \left(\frac{\partial l}{\partial t}\right)_{convergence} + \left(\frac{\partial l}{\partial t}\right)_{turb} \quad (1)$$

where the first term on the right (which will be negative by definition) represents all convergent processes that are acting to thin the layer and the second term on the right (positive) represents the diffusive effects of turbulent mixing. During the formation period, the effects of convergences exceed the diffusion by turbulence, and the sum of the two terms in Eq. 1 would be negative as the layer thins. The reverse is true during layer dissipation, and the sum in Eq. 1 would be positive. An equilibrium layer thickness will occur at the point where the broadening of the layer by turbulent diffusion just balances the effects of the convergence. The condition for layer maintenance is therefore described by

$$\left(\frac{\partial l}{\partial t}\right)_{convergence} + \left(\frac{\partial l}{\partial t}\right)_{turb} = 0 \quad (2)$$

which captures the balance between the diffusive effects of turbulence acting to increase the layer thickness and a convergence mechanism acting to collapse or thin the layer.

Considering the action of turbulent diffusion in the cross-layer direction (assuming isotropic turbulence), the broadening of the layer is governed by (*see*, e.g., Fischer et al. 1979)

$$\left(\frac{\partial l^2}{\partial t}\right)_{turb} = 2K \quad (3)$$

where K is a locally constant turbulent diffusion coefficient. Equation 3 reduces to

$$\left(\frac{\partial l}{\partial t}\right)_{turb} = \frac{K}{l} \quad (4)$$

which can be substituted into Eq. 2

$$\left(\frac{\partial l}{\partial t}\right)_{convergence} + \frac{K}{l} = 0 \quad (5)$$

which is the condition for an equilibrium layer thickness to exist.

Based on Eq. 4, the rate of layer broadening caused by turbulence decreases with layer thickness. Therefore, for layers greater than the equilibrium condition, the turbulence term in Eq. 5 (which is positive) will be reduced, and the total $\frac{\partial l}{\partial t}$ will be negative because of the effects of the convergence, assuming that the rate of convergence is independent of the layer thickness (or decreases in effectiveness as the layer thins). For layer thicknesses less than that defined by the balance in Eq. 5, $\frac{\partial l}{\partial t}$ is positive because of the increased effectiveness of turbulence relative to the convergence mechanism. As a result, we conclude that the thin layer thickness defined by Eq. 5 will be a stable equilibrium, with the exception of the case where the convergence mechanism becomes more effective as the layer thins, in which case the stability is unclear. This stability condition should enable layers to persist through the interaction of convergences and diffusion. In the following sections, we scale the first term in this equation, enabling the layer thickness to be estimated for various convergence–diffusion balances.

Straining

We begin this discussion following the work of Franks (1995), Osborn (1998), and Eckhart (1940), where the straining of an initially broad patch of scalar is described. In this case, we define the initial patch dimensions to be L_x in the horizontal and L_z in the vertical (Fig. 1a, after Eckhart 1940). We now assume that this patch is strained by a sheared velocity profile, which is described by a vertical variation in the horizontal velocity (Fig. 1a). Locally, this shear can be approximated as constant, and we define

$$\alpha = \frac{\partial U}{\partial z} \quad (6)$$

Initially, turbulent diffusion is not a significant contributor to the evolution of the patch; as the patch is strained, however, its thickness is reduced until eventually turbulent diffusion becomes important in the cross-patch direction (Fig. 1c).

The use of a constant shear and diffusion coefficient means that we are considering the local balance between straining and diffusion. The validity of this assumption will depend on the scale of the layer relative to variation in these physical parameters. Even if there is some vertical variation in these parameters, however, a first-order approximation using constant values is likely to be appropriate in defining the steady-state layer structure.

Using the parameters as defined in Fig. 1, we now consider the evolution of l, the vertical thickness of the layer, and θ, the angle the layer makes with the horizontal under the action of straining and turbulent diffusion. The initial conditions on these parameters are $l = L_z$ and $\theta = \pi/2$.

First, we consider how the straining process will lead to a thinning of the layer with time, while also tilting the layer to be more horizontal. As Franks (1995) outlined, the

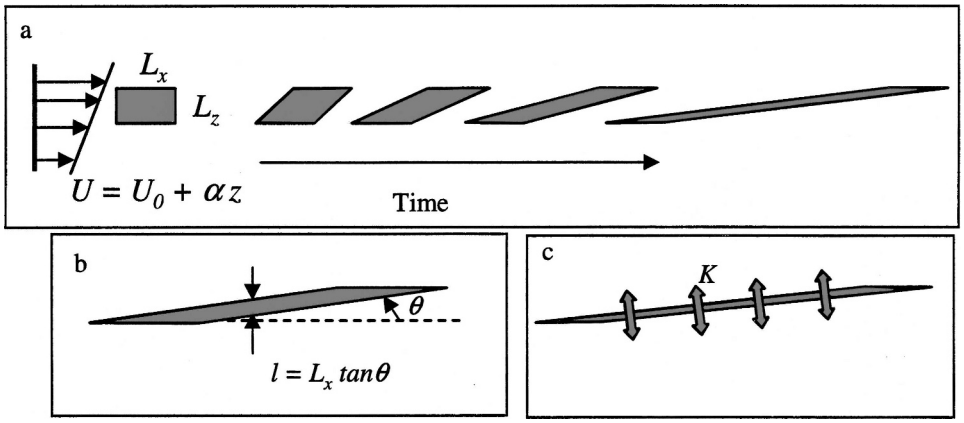

Fig. 1. A sketch of (a) the straining process and velocity shear and definition of layer parameters including (b) the layer thickness, l, the angle the layer makes with the horizontal, θ; and (c) the turbulent diffusion coefficient, K.

geometry of the layer (Fig. 1b) defines

$$l(t) = L_x \tan\theta \tag{7}$$

The action of the velocity shear manifests itself through the tilting of the angle of the layer, which asymptotically approaches zero:

$$\tan\theta = (\alpha t)^{-1} \tag{8}$$

where α is the local velocity shear, and t is time. To compare the effectiveness of straining relative to turbulent diffusion, we need to consider the rate of change of layer thickness caused by the straining. Substituting the expression for the layer angle (Eq. 8) into the equation for layer thickness (Eq. 7) and taking the time derivative gives

$$\left(\frac{\partial l}{\partial t}\right)_{strain} = L_x \frac{\partial}{\partial t}(\tan\theta) = L_x \frac{\partial}{\partial t}\left((\alpha t)^{-1}\right) = -\frac{L_x}{\alpha t^2} \tag{9}$$

This expression defines layer thickness as a function of time and initial conditions; fixed relationships between l, L_x, θ, and t (Eq. 7 and Eq. 8) and the assumption that the angle θ is small such that $\tan\theta \approx \theta$, enable us to rewrite this expression as

$$\left(\frac{\partial l}{\partial t}\right)_{strain} = -l\alpha\theta \tag{10}$$

What we find in this expression is that the thinning rate of the layer, or the effectiveness of the straining, decreases as a function of time because the layer approaches a horizontal position (i.e., θ approaches 0). If a layer were exactly horizontal, straining would no longer be effective at thinning the layer, and turbulent diffusion would act to broaden the layer. This trend is reinforced by the dependence of the rate of layer thinning on the layer thickness itself; as the layer gets thinner through time, the rate of thinning decreases. Thus, we expect that at some point in time turbulent diffusion will be able to counteract the effectiveness of straining. At this point, the broadening effects of turbulence will balance the thinning effects of the shear, and a quasi-steady state will result. Note that the term quasi-steady state is used because the layer thickness will continue to evolve due to the changing angle the layer makes with the horizontal, but from this point on, the layer thickness will be defined by a balance between turbulent diffusion and straining.

By substituting Eq. 10 into Eq. 5 and solving for the scale at which straining and diffusion balance, we have

$$l_{strain} = \sqrt{\frac{K}{\alpha\theta}} \tag{11}$$

This result defines a scale estimate for layer thickness caused by a balance between straining and turbulent diffusion, which we have defined as l_{strain}. In later sections, we will compare this layer scale to similar estimates for buoyancy- and motility-induced convergences. First, however, we describe the unsteady development of the layer under the action of straining.

Discussion of time evolution—Using both the geometric analysis summarized in Fig. 1 and the scaling results of the previous section, we can now define the time development of the layer thickness under the combined action of straining and turbulent diffusion. Initially, the patch is described by vertical dimension L_z; after a time $t_{start} = L_x/(L_z\alpha)$ (to account for the dimensions of the initial patch), the layer thickness is given by

$$l(t) = \frac{L_x}{\alpha t} \tag{12}$$

where we have assumed that during this initial phase the development is dominated by the straining.

We now argue that the layer will reach a quasi-steady state when the pure straining expression (Eq. 12) approaches the balanced expression (Eq. 11). Equality of these two expressions (and assuming $\tan\theta \approx \theta$ in Eq. 8) leads to the definition of a timescale for the diffusion-

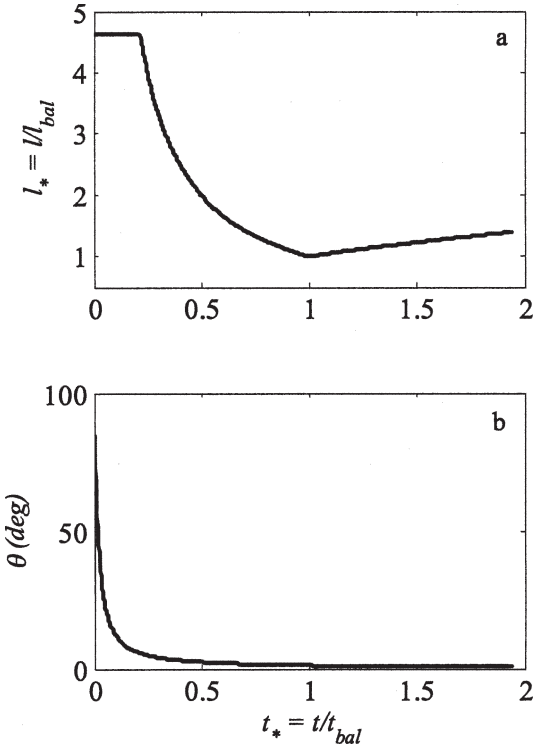

Fig. 2. Evolution of (a) the layer thickness scale and (b) layer angle, including a transition from pure straining (for $t < t_{bal}$) to a straining–diffusion balance (for $t > t_{bal}$). Point of intersection defines when processes will be in balance ($t = t_{bal}$).

straining balance to develop:

$$t_{bal} = \left(\frac{L_x^2}{K\alpha^2}\right)^{1/3} \tag{13}$$

Before this time, straining is acting to thin the layer; after this time, the layer gradually broadens because of the decreasing effectiveness of straining. As a result, the minimum layer thickness occurs at this time, and is given by

$$l_{\min} = \left(\frac{KL_x}{\alpha}\right)^{1/3} \tag{14}$$

In Fig. 2, we present the time evolution of both the layer thickness and the angle with the horizontal as functions of time based on Eq. 7 and Eq. 8. It can be seen that the angle monotonically decreases toward zero, with a representative timescale of $1/\alpha$. The layer thickness first undergoes a reduction in lengthscale because of the action of straining until it reaches a condition at which straining and turbulent diffusion are in balance. The angle that the layer makes with the horizontal at this transition is given by

$$\tan\,\theta_{bal} = \frac{1}{\alpha t_{bal}} = \left(\frac{K}{\alpha L_x^2}\right)^{1/3} \tag{15}$$

Using the fact that the angle is likely to be quite small when this balance occurs, we conclude that

$$\theta_{bal} = \left(\frac{K}{\alpha L_x^2}\right)^{1/3} \tag{16}$$

For times greater than t_{bal} or angles less than θ_{bal}, the layer thickness evolves as defined by Eq. 11, which represents a balance between straining-induced convergence and turbulent diffusion.

With this result, we can describe the evolution of layer thickness under the action of steady shear as

$$l(t) = L_z \quad \text{for } t < t_{start} \tag{17}$$

$$l(t) = \frac{L_x}{\alpha t} \quad \text{for } t_{start} < t < t_{bal} \tag{18}$$

$$l(t) = \sqrt{K/(\alpha\theta)} \quad \text{for } t > t_{bal} \tag{19}$$

These relationships are summarized in Fig. 2. After some initial period (t_{start}) to account for the initial patch dimensions, the patch is strained by the velocity shear, becoming thinner in time as described by Eq. 12. After that point, the detailed analysis of the interaction between straining and turbulent diffusion predicts a gradual increase in layer thickness (Eq. 11, Fig. 2a).

Motility

For zooplankton and some phytoplankton (specifically dinoflagellates), swimming behavior is frequently invoked to explain the development and maintenance of thin layers (Rines et al. 2002; Genin et al. 2005). To establish the rate of convergence created by species motility, we define the vertical velocity to be

$$W = -w_s \quad \text{for } z > z_0 \tag{20}$$

$$W = w_s \quad \text{for } z < z_0 \tag{21}$$

This assumes that the swimming velocity is constant (defined by w_s) and is oriented toward the center of the layer (at z_0). Frequently a hyperbolic tangent formulation for swimming speed is assumed (*see* Franks 1992), which would result from a more diffused "target" layer. From a scaling perspective, the lengthscale contained in the hyperbolic tangent formulation brings an explicit thickness to the analysis; to focus on the convergence–diffusion interaction, we will use the constant formulation in Eq. 20 and Eq. 21 so as to define a lengthscale for the layer without specifying other layer thicknesses.

The rate of collapse of a patch under just the action of a convergent vertical migration is given by the swimming velocity:

$$\left(\frac{\partial l}{\partial t}\right)_{swim} = -w_s \tag{22}$$

Balancing this rate of convergence with the turbulent divergence results in

$$\left(\frac{\partial l}{\partial t}\right)_{swim} + \left(\frac{\partial l}{\partial t}\right)_{turb} = -w_s + \frac{K}{l} = 0 \quad (23)$$

which defines a thickness of the layer as

$$l_{swim} = \frac{K}{w_s} \quad (24)$$

A direct comparison of the influence of swimming and straining can be considered through the ratio of these scales:

$$\left(\frac{l_{strain}}{l_{swim}}\right)^2 = \frac{w_s^2}{K\alpha\theta} \quad (25)$$

This defines a critical condition on the swimming velocity at which these two processes are of equal importance:

$$w_s^{crit} = \sqrt{K\alpha\theta} \quad (26)$$

For w_s greater than this value, swimming is more effective than the shear-driven convergence presented in the previous section at maintaining a coherent thin layer. As was reported by Genin et al. (2005) copepods were able to effectively counter vertical velocities as large as 10 body lengths per second.

It is important to note that this swimming analysis assumes that the individuals swim with constant speed toward an infinitesimally thin "target" layer and will therefore require some ambient layer structure, established through other mechanisms, for it to be effective (Genin et al. 2005).

Buoyancy

A mechanism that is frequently invoked to explain layer formation and maintenance is particle buoyancy and the creation of layers on pycnoclines (Franks 1992). In this case, a particle of density ρ_p is retained along an isopycnal of equal density ($\rho_w = \rho_p$) by a buoyancy-induced restoring force. If the particle is displaced from this equilibrium level, the density difference between the particle and the surrounding water forces the particle back toward its equilibrium position. In the low Reynolds number limit, Stokes' law can be used to define the velocity with which it will move back toward its equilibrium position:

$$V_{settle} = -\frac{\Delta\rho\, gD^2}{\rho_0\, 18\nu} \quad (27)$$

where $\Delta\rho$ is the difference between the particle density and the surrounding water density, D is the particle diameter (assuming a spherical particle), g is the gravitational acceleration, and ν is the molecular viscosity of water.

If we now consider a particle that is at equilibrium in the center of a linear density profile (at $z = z_0$), then the density difference is related to the position of the particle as

$$\frac{\Delta\rho}{\rho_0} g = -\frac{g}{\rho_0}\frac{\partial\rho}{\partial z}(z - z_0) = N^2(z - z_0) \quad (28)$$

where $N^2 = -\frac{g}{\rho_0}\frac{\partial\rho}{\partial z}$ is the buoyancy frequency. This relationship results in a vertical particle velocity of

$$V_{settle} = W = -\frac{N^2D^2}{18\nu}(z - z_0) \quad (29)$$

Scaling $(z - z_0)$ with the layer thickness leads to

$$V_{settle} = W = -\frac{N^2D^2}{18\nu} l \quad (30)$$

Just as in the case of swimming, this settling velocity is exactly equal to the rate of change of layer thickness caused by the effects of buoyancy. If this convergence mechanism is to be effective in establishing a steady layer structure, this rate of layer collapse must balance the rate of expansion of the layer by turbulence, which leads to

$$-\frac{N^2D^2}{18\nu} l + \frac{K}{l} = 0 \quad (31)$$

Solving this relationship for layer thickness results in

$$l_{buoy} = \sqrt{\frac{18K\nu}{N^2D^2}} \quad (32)$$

The comparison between buoyancy and straining mechanisms can be quantified by considering the ratio of the layer thicknesses defined by Eq. 11 and Eq. 32, which we will refer to as l_{strain} and l_{buoy}, respectively. That is,

$$\left(\frac{l_{strain}}{l_{buoy}}\right)^2 = \frac{N^2D^2}{18\nu\alpha\theta} \quad (33)$$

Because α is the velocity shear, we can rewrite this equation using the gradient Richardson number, $Ri_g = \frac{N^2}{\alpha^2}$:

$$\left(\frac{l_{strain}}{l_{buoy}}\right)^2 = Ri_g \frac{D^2\alpha}{18\nu\theta} \quad (34)$$

Focusing on the gradient Richardson number, we can establish a critical value based on Eq. 34 at which the effectiveness of buoyancy is equivalent to that of straining:

$$Ri_g^{crit} = \frac{18\nu\theta}{D^2\alpha} \quad (35)$$

For values of Ri_g less than this value, l_{strain} is smaller than l_{buoy}, which means that the straining process is more

important in defining the layer thickness. If Ri_g is greater than $Ri^{crit}{}_g$, then buoyancy is expected to be the dominant process. We note that this critical threshold does not depend on the turbulent diffusion coefficient, K, and is therefore estimable from mean flow variables, provided a rough estimate of the layer inclination and particle diameter is available.

Other mechanisms

The framework presented in the introduction to this section, which evaluates the competition between convergent and divergent processes in establishing the layer thickness, is applicable to many other processes that are not presented here. We have limited our development in this article to these three basic convergent mechanisms (straining, motility, and buoyancy) which are frequently invoked in the analysis of thin layers, and we have assumed that they each act independently. It is probable that in many layers more than one convergence mechanism is responsible for the formation and maintenance of the layer. For example, settling of particles into a layer, or downward migration into a layer, could dominate the convergence on the upper side of the layer, whereas straining provides the convergence mechanism to preserve the sharpness of the lower side of the layer. In this case, the analysis of convergence and defining the resulting rate of thinning of the layer for use in Eq. 5 would rely on the average of the two convergence mechanisms. Although a detailed development of this analysis is beyond the scope of this manuscript, the framework presented here would be readily applicable.

In addition to considering each convergence mechanism separately, we are making the simplifying assumption that these convergent processes are essentially homogeneous. As such, we are not, at this time, including other mechanisms for layer formation, such as spatially variable growth or grazing rates.

Our analysis framework would also, of course, permit other divergent mechanisms to be considered beyond the homogeneous turbulent diffusion discussed here. Examples of other dissipative mechanisms could include diffusive (undirected) swimming, out migration from the layer (directed swimming), or buoyancy regulation. In the case of each of these other mechanisms, a velocity scale can be defined that defines the rate of layer thinning or thickening, which can then be used in the lengthscale analysis described here.

Finally, internal wave motions could be either a convergent or divergent process, depending on whether isopycnals are being compressed or expanded by the waves at a point in time. These effects could easily be incorporated into our framework through the addition of an additional time derivative term to account for the waves; this analysis is not presented in this article.

Detailed analysis of cross-layer structure

The previous results define a scale estimate for layer thickness for the balance between turbulent diffusion and three different convergence mechanisms: straining, motility, and buoyancy. Those scaling results are used in the next section to differentiate between the various convergence mechanisms. In this section, we note that in certain cases, for each of the balances previously described, a more detailed solution for the structure of the layer is possible.

A common element in many of the observations of thin layers is that the concentration in the layer tends to have a sharp maximum around the center of the layer (*see*, for example, Rines et al. 2002, fig. 5). This is in direct contrast to the Gaussian shape that would result from typical diffusive mixing processes (Fischer et al. 1979), even in the presence of growth. To be more specific, many observed layers have a discontinuity in the gradient of the concentration, with the vertical gradient of concentration reaching a maximum near the maximum in concentration; Gaussian distributions are characterized by a zero-gradient at the maximum concentration. Clearly, the dynamical balance that is establishing and maintaining the vertical structure of these layers cannot be described with a purely diffusive process, even if local growth is included. Instead, a convergence mechanism is required to maintain the sharply peaked structure that is evident in many observations.

Straining–diffusion balance—In a reference frame rotated to coincide with the axis of the layer, the cross-layer velocity is convergent and proportional to distance from the center of the layer (Garrett 1983; Townsend 1951). For our case, assuming that the angle the layer makes with the horizontal (θ) is small, the cross-layer velocity (W_l) can be written as

$$W_l = -(U_0 + \alpha z_l)\theta \tag{36}$$

where U_0 is the mean velocity of the layer, and z_l is the cross-layer coordinate. In Garrett's (1983) analysis, the interaction of straining and diffusion results in a two-dimensional Gaussian distribution. The advection–diffusion equation can be reduced to the one-dimensional, cross-layer competition between the convergence and turbulent diffusion for a highly anisotropic situation such that the along-layer concentration gradients can be neglected, which may be appropriate away from the lateral limits of the layer. Using the velocity in Eq. 36, we can integrate the advection–diffusion equation across the layer to get

$$C(z_l) = C_0\left(1 - \left|erf\left(\frac{z_l}{\sqrt{2K/(\alpha\theta)}}\right)\right|\right) \tag{37}$$

where z_l is the cross-layer coordinate; K, α, and θ are as defined above; and C_0 is the maximum concentration in the layer. We expect this solution to hold in the cross-layer direction (z_l), which is nearly vertical for small angles θ. Importantly, this solution will only be valid away from the edges of the layer in the along-layer direction because of a necessary assumption of along-layer uniformity in developing this solution.

This profile is plotted in Fig. 3 and is seen to have a sharply peaked maximum at the center of the layer, which

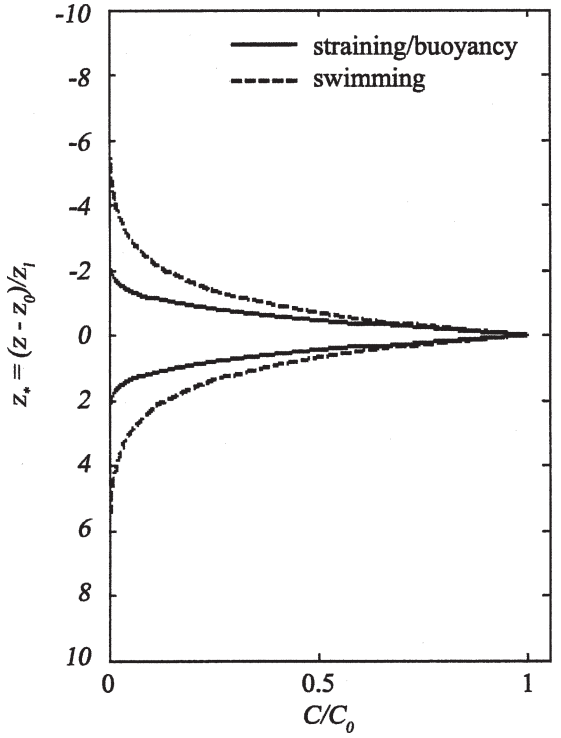

Fig. 3. A comparison of normalized straining and buoyancy solution (solid line) with normalized swimming solution (dotted line).

is consistent with the observations of thin layers in the coastal ocean (Dekshenieks et al. 2001; Rines et al. 2002). Using our previously defined straining lengthscale (Eq. 11), and z_0 as the center of the layer, then the functional form of the solution collapses to

$$C(z) = C_0\left(1 - \left|erf\left(\frac{z - z_0}{l_{strain}}\right)\right|\right) \tag{38}$$

Motility–diffusion balance—With the vertical velocity given by Eq. 20 and Eq. 21, the advection–diffusion equation in the cross-layer direction can be solved in each half-plane through integration, resulting in

$$C(z) = C_0 e^{-\frac{w_s}{K}|z - z_0|} \tag{39}$$

where z_0 is the center of the layer, K is the diffusion coefficient, and C_0 is the centerline concentration of the layer. For this exponential decay of concentration from the center of the layer, the characteristic thickness for the layer in this case is given by Eq. 24, that is $l_{swim} = \frac{K}{w_s}$.

In Fig. 3, this profile is compared directly with that created by the straining mechanism for the case where the layer thickness of the two approaches is equivalent (that is, $l_{swim} = l_{strain}$). Whereas there is a difference between the two curves when $l_{swim} = l_{strain}$, the two curves would be nearly identical if a concentration profile were used to estimate the underlying lengthscales (l_{swim} would be less than l_{strain} because of the mathematical form of the two solutions).

Buoyancy–diffusion balance—Examining the rate of layer collapse caused by buoyancy (Eq. 30), we see that the effective convergence velocity is proportional to cross-layer position, just as in the case of straining (Eq. 36). As a result, the buoyancy convergence has the same mathematical form as the straining-induced convergence, and the solution from Eq. 37 can be applied to this case with l_{buoy} replacing l_{strain}:

$$C(z) = C_0\left(1 - \left|erf\left(\frac{z - z_0}{l_{buoy}}\right)\right|\right) \tag{40}$$

This profile shape is exactly equivalent to that for straining in Fig. 3, so a comparison of these two convergence mechanisms would rely on the evaluation of the lengthscales, as outlined in the previous section.

Example application: East Sound 1996

To illustrate the application of the framework developed in this work, we apply it to observations of thin layers, which include coincident measurements of both shear and stratification. By applying the expressions for cross-layer scale (Eq. 11 and Eq. 32), we can evaluate the convergence–divergence balance implied by the observed layers.

In 1996, a comprehensive data set describing layer development was collected in East Sound, Washington (Dekshenieks et al. 2001; Alldredge et al. 2002; Rines et al. 2002). In a paper describing these observations, Dekshenieks et al. (2001) provide a summary of layer thickness, density gradient, and velocity shear. Table 1 summarizes the data from several representative events, which consist of a series of observations of the same layer. The values in this table represent mean values over the period of layer observation. Variations around these mean values are summarized in Figs. 4 and 5 by showing the range of values observed in the parameters. In Fig. 4, the basic characteristics of the layers for each event are presented, including the observed layer thickness (Fig. 4a), the buoyancy frequency squared (N^2, Fig. 4b), and the shear squared (S^2, Fig. 4c). In each case, the shear and stratification vary across a relatively narrow range as does the layer thickness, with the exception of event B. Across events, however, there is greater variation in these parameters.

We now consider the dynamics of each of these events in the context of the framework developed here. We first pursue an analysis of layer divergence caused by turbulent mixing, for which we require estimates of turbulent mixing coefficients. We start this analysis with the estimation of the Thorpe (or overturning) scale (Thorpe 1977), which is calculated as the mean displacement scale (based on the sorting of the density profile) over the segment of the density profile occupied by an observed thin layer. As seen in Fig. 5a, the Thorpe scale is much smaller than the observed layer thicknesses and, again with the exception of event B, varies over a relatively narrow range within each event.

Under the assumption that the overturning scale is equal to the Ozmidov scale (*see,* e.g., Gregg 1987), the turbulent

Table 1. Observed layer thickness from Dekshenieks et al. (2001) and implications of frameworks presented here. Turbulent parameters, including the Thorpe scale, the dissipation rate, and the diffusion coefficient, are discussed in the text. The last two columns report the values of particle diameter and layer angle required for the buoyancy and straining mechanisms to balance turbulent diffusion, respectively.

Event	Layer numbers (Dekshenieks 2001)	Average layer thickness (cm)	L_t (cm)	N^2 (s^{-2})	S^2 (s^{-2})	ε, $L_t^2 N^3$ (W kg^{-1})	K, $\gamma_{mix}\varepsilon N^{-2}$ (cm^2 s^{-1})	dl/dt_{turb} (cm s^{-1})	D_{bal} (cm)	Θ_{bal}
A	50, 52, 55, 57	90.25	3.6	2.7×10^{-3}	2.1×10^{-3}	1.8×10^{-7}	1.0×10^{-1}	5.6×10^{-4}	2.0×10^{-2}	1.4×10^{-4}
B	51, 53, 56, 58, 61	71.4	4.155	1.5×10^{-3}	1.8×10^{-3}	1.0×10^{-7}	1.0×10^{-1}	7.0×10^{-4}	3.4×10^{-2}	2.3×10^{-4}
C	65, 68, 71, 72	50	2.053	7.1×10^{-3}	1.5×10^{-4}	2.5×10^{-7}	5.3×10^{-2}	5.3×10^{-4}	1.6×10^{-2}	8.8×10^{-4}
D	91, 93, 95, 96, 100	143.5	7.987	3.3×10^{-4}	1.6×10^{-4}	3.7×10^{-8}	1.7×10^{-1}	6.0×10^{-4}	4.8×10^{-2}	3.3×10^{-4}

dissipation rate can be estimated as

$$\varepsilon = L_t^2 N^3 \tag{41}$$

The assumption that the overturning scale is nearly equal to the Ozmidov scale has been confirmed by observations (Dillon 1982) and is consistent with turbulence at maximal efficiency (Ivey and Imberger 1991). In other words, we are assuming that the turbulence is in equilibrium with the stratification (Holt et al. 1992), and that the turbulent Froude number is unity (Ivey and Imberger 1991). The dissipation rate for each event is presented in Fig. 5b. In all cases, the dissipation rate varies from about 5×10^{-7} W kg^{-1} to 1×10^{-8} W kg^{-1}. Once again, event B shows the widest range of conditions. It is important to note here the broad uncertainty range associated with these estimates. Uncertainty in this estimate of the dissipation rate is caused by three factors: inherent uncertainty in the

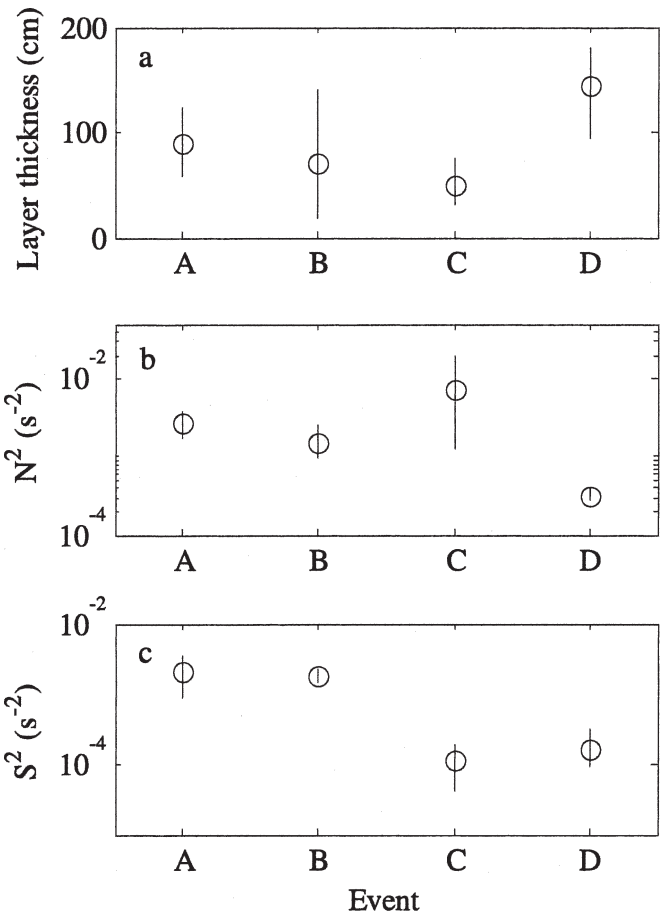

Fig. 4. Characteristics of layers observed in East Sound 1996. (a) Observed layer thickness, (b) buoyancy frequency squared, and (c) shear squared associated with each event. *See* Table 1 for definition of events.

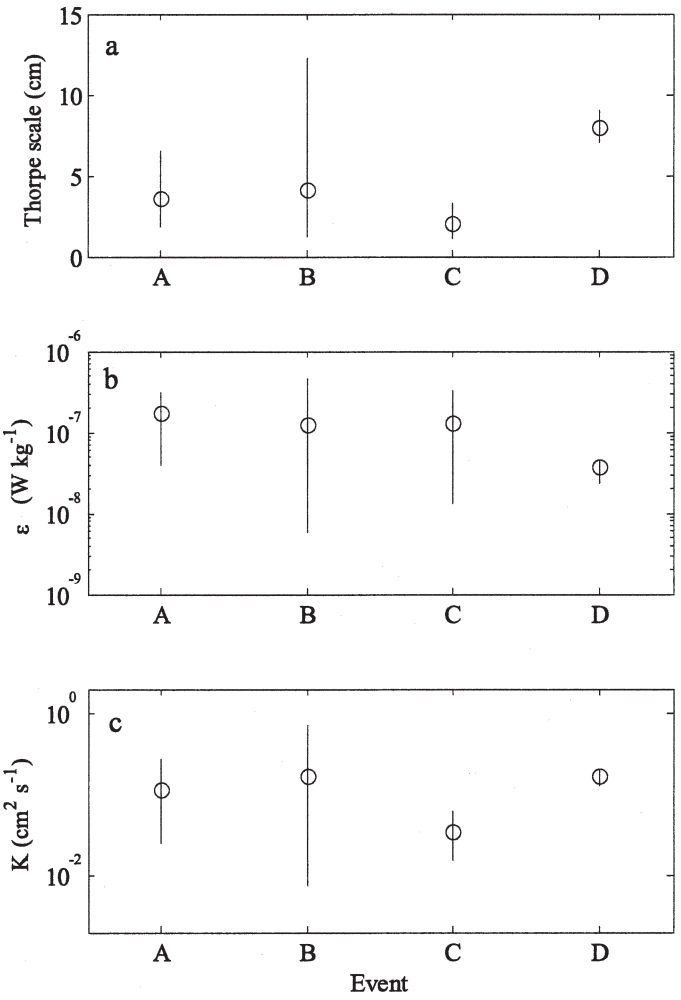

Fig. 5. Turbulence characteristics associated with layers observed in East Sound 1996 (*see* Table 1 for event definitions). (a) Observed Thorpe scale, (b) estimated dissipation rate of turbulent kinetic energy, and (c) estimated turbulent diffusion coefficient.

estimate of the Thorpe scale, an uncertain relation between the Thorpe scale and the Ozmidov scale, and natural intermittency and variability in the local dissipation rate. As such, the uncertainty limits presented in Fig. 5b are probably the lower limit for these uncertainties, but are illustrative of the errors in the estimates.

Using this estimate of the dissipation rate, and assuming a local balance between shear production, dissipation rate, and buoyancy flux, we can estimate an upper-bound on the turbulent diffusion coefficient using (Osborn 1980)

$$K = \gamma_{mix} \frac{\varepsilon}{N^2} \tag{42}$$

The specification of the mixing efficiency (γ_{mix}) should depend on the state of the turbulence through, for example, the turbulent Froude number (Ivey and Imberger 1991) and will introduce additional uncertainty into the estimate of divergence by the turbulence. Around a turbulent Froude number of 1, however, the mixing efficiency is at or near its maximum value of 0.2 ($R_f = 0.15$, which is slightly lower than Ivey and Imberger 1991), which is consistent with the formulation proposed by Osborn (1980) and applied regularly in the oceanic thermocline. Based on this assumption of the mixing efficiency, turbulent diffusion coefficients in the range of 0.01 $cm^2\ s^{-1}$ to 1 $cm^2\ s^{-1}$ are estimated for each of the events considered (Fig. 5c).

Using the mean values of these parameters within each event, as summarized in Table 1, we now apply the framework developed here. First, based on the turbulent diffusivity, we calculate the rate of layer broadening caused by turbulent mixing, which is reported in column nine of Table 1. These layer growth rates must be offset by a convergence mechanism in order for a steady layer thickness to result. For the species observed in East Sound, motility was unlikely to be a significant mechanism for convergence (Rines et al. 2002), so we now consider the role that the buoyancy and straining mechanisms could have played in layer formation and maintenance.

In each of these cases, there is one parameter in the formulation of the convergence mechanism that is unknown; for buoyancy, the effective particle diameter is uncertain, whereas for straining, the layer angle relative to the local advection is unknown. Rather than specifying these parameters based on independent observations or analysis, we instead define the value of each of these parameters that would result in an equilibrium between that mechanism and turbulent diffusion. The equilibrium particle diameter implied by the buoyancy mechanism is shown in column 10 of Table 1; the angle of layer inclination required for the straining mechanism is shown in column 11 of Table 1. Remarkably, although the ambient shear and stratification varied widely between these events, the particle diameter required to offset the effects of turbulence is quite constant across events and is not too different from independent estimates of particle size (0.04 cm). The required angle of inclination is also relatively uniform across events, and the values that result are physically plausible based on the observed layer duration, but without independent measurements of the inclination of the layer, this result cannot be evaluated.

Together, we conclude that the buoyancy and straining mechanisms are candidates for the maintenance of the observed layers in East Sound. In this case, without independent estimates of the particle diameter and the layer angle, the analysis cannot distinguish between them. The framework presented here does, however, provide a method within which the various convergence mechanisms can be quantitatively compared and analyzed.

Discussion

The analysis presented in this article provides a framework for incorporating turbulent mixing into the analysis of thin-layer structure and dynamics. We extend Franks' (1995) analysis of kinematic straining to include cross-layer diffusion using a scaling approach that characterizes the unsteady development of a layer under the action of a sheared velocity profile. Similar scaling analysis for the action of motility and buoyancy results in scale estimates for layer thickness under each of the three candidate balances. A more detailed analysis of the cross-layer structure shows that the interaction of these convergence mechanisms with turbulent diffusion results in a sharply peaked concentration profile that is consistent with the observations. It is important to note that the relative importance of each of these convergence mechanisms will depend on the local conditions (stratification, shear, particle diameter and motility, and layer inclination) that are forcing the layer at a point in time. As a result, we expect that the mechanism dominating layer formation and maintenance may, in fact, change as the layer evolves.

One of the implications of the framework itself is the expectation of a finite lifetime for layers produced by straining. As straining proceeds, the angle of inclination of the layer continues to approach zero, which makes straining less effective as a convergence mechanism. In fact, the time behavior presented in Fig. 2 shows that for times greater than the balancing point (denoted t_{bal}), the layer thickness actually increases. Thus, a change in the level of turbulent diffusion (or other divergence mechanisms) is not required for the layer to dissipate, even if the straining continues indefinitely. The other convergence mechanisms considered here (motility and buoyancy), however, could maintain a thin layer indefinitely and, as a result, increases in layer divergences could be more important to the dissipation of these layers.

Although we have presented them as separate processes here, convergences and divergences cannot be entirely decoupled because of the interaction of shear, stratification, and turbulent mixing. As outlined above, the comparison between the importance of the straining and buoyancy convergence mechanisms results in a gradient Richardson number criteria, with buoyancy becoming more important for large Richardson numbers. At the same time, however, we expect an inverse relationship between the gradient Richardson number and turbulent mixing through reductions in turbulent energy and perhaps the mixing efficiency (or, equivalently, the flux Richardson number). As a result, in strongly stratified conditions, the buoyancy–diffusion mechanism is reinforced by the re-

duction in turbulent diffusion. The straining–diffusion balance, however, is characterized by a negative feedback because of the expectation for shear to provide a production mechanism for turbulence, which would both diffuse the layer and reduce the shear itself. For strongly sheared flows, therefore, the competition between the straining of the patch and the production of turbulence by the shear must be considered.

During the dissipation phase of the layer, however, the buoyancy and straining mechanisms are reduced by the turbulent mixing of momentum and density, which reduces the shear and stratification that may be providing the required convergence for layer maintenance. As a result, mixing events that act to dissipate the layer act to both disperse the layer and reduce the convergence mechanism that is maintaining the layer. For layers maintained by motility, however, the connection between turbulent mixing and changes to the convergence mechanism is less clear. Although there is some evidence that individuals may swim to escape turbulent regions (Franks 2001), the net effect on the layer structure cannot be established at this time.

Application of the framework to observations from East Sound suggest that the buoyancy mechanism and the straining mechanism are likely to contribute to the maintenance of the observed layers, at least to within the uncertainty in the turbulence analysis. Whereas swimming is certainly relevant for copepods (Genin et al. 2005), for the non-motile species considered here, we cannot distinguish between the buoyancy and straining mechanisms with the existing observations.

The formal development of this framework also guides future data collection efforts. The variation of layer thickness at short timescales (minutes to hours) can now be analyzed in the context of the mechanisms that lead to changes in layer thickness. Simultaneous observation of turbulence parameters, particularly turbulent dissipation rate, with the more traditional descriptions of layer structure and variability can be integrated into a more complete description of layer formation, maintenance, and eventually, dissipation. To develop detailed comparisons of the roles of various convergence mechanisms, however, other auxiliary measurements would be extremely valuable, and perhaps necessary. In the case discussed here, independent knowledge of the particle sizes, perhaps based on multifrequency acoustics, and layer angle of inclination, which would require synoptic surveys, would enable a more complete evaluation of the convergence mechanism responsible for the observed layers.

References

Cowles, T. J., and R. A. Desiderio. 1993. Resolution of biological microstructure through in situ fluorescence emission spectra: An oceanographic application using optical fibers. Oceanography **6:** 105–111.

———, ———, J. N. Moum, M. L. Myrick, D. Garvis, and S. M. Angel. 1990. Fluorescence microstructure using a laser/fiber optic profile. Ocean Optics X, Proceedings of SPIE. **1302:** 336–345.

Dekshenieks, M. M., P. L. Donaghay, J. M. Sullivan, J. E. B. Rines, T. R. Osborn, and M. S. Twardowski. 2001. Temporal and spatial occurrence of thin phytoplankton layers in relation to physical processes. Mar. Ecol. Progr. Ser. **223:** 61–71.

Dillon, T. M. 1982. Vertical overturns—A comparison of Thorpe and Ozmidov length scales. J. Geophys. Res. Ocean. Atmos. **87:** 9601.

Eckhart, C. 1940. The thermodynamics of irreversible processes 2. Fluid Mixtures. Phys. Rev. **58:** 269–275.

Fischer, H. G., E. J. List, R. C. Y. Koh, J. Imberger, and N. H. Brooks. 1979. Mixing in inland and coastal waters. Academic Press.

Franks, P. J. S. 1992. Sink or swim—Accumulation of biomass at fronts. Mar. Ecol. Progr. Ser. **82:** 1–12.

———. 1995. Thin layers of phytoplankton: A model of formation by near-inertial wave shear. Deep-Sea Res. **42:** 75–91.

———. 2001. Turbulence avoidance: An alternate explanation of turbulence-enhanced ingestion rates in the field. Limnol. Oceanogr. **46:** 959–963.

Garrett, C. 1983. On the initial streakiness of a dispersing tracer in two- and three-dimensional turbulence. Dyn. Atmos. Oceans. **7:** 265–277.

Genin, A., J. S. Jaffe, R. Reef, C. Richter, and P. J. S. Franks. 2005. Swimming against the flow: A mechanism of zooplankton aggregation. Science **308:** 860–862.

Gibson, C. H. 1980. Fossil temperature, salinity and vorticity in the ocean,, *In* J. C. T. Nihoul [ed.], Marine turbulence. Elsevier.

Gregg, M. C. 1987. Diapycnal mixing in the thermocline: A review. J. Geophys. Res. **92:** 5249–5286.

Holliday, D. V., R. E. Pieper, C. F. Greenlaw, and J. K. Dawson. 1998. Acoustical sensing of small scale vertical structures in zooplankton assemblages. Oceanography **11:** 18–23.

Holt, S. E., J. R. Koseff, and J. H. Ferziger. 1992. The evolution of turbulence in the presence of mean shear and stable stratification. J. Fluid Mech. **237:** 499–539.

Ivey, G. N., and J. Imberger. 1991. On the nature of turbulence in a stratified fluid. Part I: The energetics of mixing. J. Phys. Oceanogr. **21:** 650–658.

McManus, M. A., O. M. Cheriton, P. J. Drake, D. V. Holliday, C. D. Storlazzi, P. L. Donaghay, and C. F. Greenlaw. 2005. The effects of physical processes on the structure and transport of thin zooplankton layers in the coastal ocean. Mar. Ecol. Progr. Ser. **301:** 199–215.

———, and others. 2003. Changes in characteristics, distribution and persistence of thin layers over a 48-hour period. Mar. Ecol. Progr. Ser. **261:** 1–19.

Osborn, T. R. 1980. Estimates of the local rate of vertical diffusion from dissipation measurements. J. Phys. Oceanogr. **10:** 83–89.

———. 1998. Finestructure, microstructure and thin layers. Oceanography **11:** 36–43.

Rines, J. E. B., P. L. Donaghay, M. M. Dekshenieks, J. M. Sullivan, and M. S. Twardowski. 2002. Thin layers and camouflage: Hidden *Pseudo-nitzschia* spp. (Bacillariophyceae) population in a fjord in the San Juan Island, Washington, USA. Mar. Ecol. Progr. Ser. **225:** 123–137.

Thorpe, S. A. 1977. Turbulence and mixing in a Scottish loch. Phil. Trans. R. Soc. London Ser. A **286:** 125–181.

Townsend, A. A. 1951. The diffusion of heat spots in isotropic turbulence, Proc. R. Soc. London Ser. A **209:** 418–430.

Received: 2 May 2006
Accepted: 27 November 2006
Amended: 27 January 2007